Available online at www.sciencedirect.com

ScienceDirect

Ceramics International 36 (2010) 1825–1829

CERAMICS INTERNATIONAL

www.elsevier.com/locate/ceramint

Surfactant-free hydrothermal synthesis and characterization of single-crystal $K_2V_8O_{21}$ nanobelts

J.N. An [a], C.Y. Xu [a,b,c,*], L. Zhen [a,c,**], Y.D. Huang [b]

[a] School of Materials Science and Engineering, Harbin Institute of Technology, Harbin 150001, China
[b] School of Chemical Engineering, Harbin Institute of Technology, Harbin 150001, China
[c] MOE Key Laboratory of Micro-systems and Micro-structures Manufacturing, Harbin Institute of Technology, Harbin 150001, China

Received 12 November 2009; received in revised form 22 February 2010; accepted 14 March 2010
Available online 28 April 2010

Abstract

Single-crystal $K_2V_8O_{21}$ nanobelts were prepared from the reaction between V_2O_5 and $KHSO_4$ under hydrothermal condition using no surfactant or template. The synthesized nanobelts were characterized by X-ray diffraction, X-ray photon-electron spectrometry, scanning electron microscopy, and transmission electron microscopy. The nanobelts are single-crystalline in nature, and have typical width of 100–500 nm, thickness of less than 100 nm and length up to a few tens of microns. The effects of solution concentration, reaction temperature and molar ratio of K and V on the morphology and phase component of the obtained products have been investigated. The possible formation mechanism was also discussed.

Keywords: Nanobelts; Vanadates; Hydrothermal synthesis

1. Introduction

Vanadium pentoxide and its derivative compounds exhibit a wide range of practical applications such as humidity sensors, electrochromic devices, and cathodic electrodes for lithium batteries, due to their unique structural flexibility combined with chemical and physical properties. Some of these properties largely depend on the morphology and size of the product synthesized by using different approaches. This inspires chemists and materials scientists to explore new methods for the synthesis of one-dimensional (1D) nanostructured vanadates. A series of metal vanadates 1D nanostructures have been synthesized based on the hydrothermal route. For example, Yu et al. first reported a general method for the synthesis of $Na_2V_6O_{16}\cdot 3H_2O$ single-crystal nanobelts based on hydrothermal reaction-crystallization between V_2O_5 and NaF [1]. They also prepared NaV_6O_{15} nanowires and nanoneedles by using different sodium salts [2,3]. Qian and co-workers successfully fabricated single-crystal $CaV_6O_{16}\cdot 3H_2O$ nanoribbons [4] and MnV_2O_6 nanobelts [5] from the reaction between metal chlorides and NH_4VO_3 under hydrothermal conditions in the presence of sodium dodecyl sulfate (SDS) as soft templates or HF as acidifying agent, respectively. Several kinds of silver vanadates 1D nanostructures, for example, $Ag_2V_4O_{11}$ nanobelts [6], $Ag_{0.33}V_2O_5$ nanowires [7], $AgVO_3$ nanoribbons [8,9], have been successfully prepared also by hydrothermal method. Bismuth vanadates ($BiVO_4$) nanofibrous arrays were synthesized by a hydrothermal method [10]. Despite these progresses in the synthesis of different kinds of vanadates 1D nanostructures, there has been only a few works on the synthesis of potassium vanadates 1D nanostructures. For example, Wang et al. [11] developed a solvothermal route to synthesize $K_2V_3O_8$ nanorods via the reduction of V_2O_5 using ethanol as the reducing agent as well as the solvent.

$K_2V_8O_{21}$, a high vanadium content compound in K_2O–V_2O_5 system, was first reported by Illarionov et al. [12]. Later, Lukacs et al. [13] and Kato et al. [14] also reported the synthesis and X-ray diffraction data of $K_2V_8O_{21}$, both of which are different

---

* Corresponding author at: School of Materials Science and Engineering, Harbin Institute of Technology, Harbin 150001, China.
Tel.: +86 451 8641 2133; fax: +86 451 8641 3922.
** Corresponding author at: School of Materials Science and Engineering, Harbin Institute of Technology, P.O. Box 433, Harbin 150001, China.
Tel.: +86 451 8641 2133; fax: +86 451 8641 3922.
E-mail addresses: cy_xu@hit.edu.cn (C.Y. Xu), lzhen@hit.edu.cn (L. Zhen).

0272-8842/$36.00 © 2010 Elsevier Ltd and Techna Group S.r.l. All rights reserved.
doi:10.1016/j.ceramint.2010.03.031

from that reported by Illarionov [15]. This difference might be attributed to the different synthetic conditions as well as different raw materials. For example, Kato et al. prepared $K_2V_8O_{21}$ crystal by melting stoichiometric mixture of $KHCO_3$ and V_2O_5 at 550 °C for 30 min in air followed by slow cooling, while Lukacs et al. used KVO_3 and V_2O_5 as raw materials. Note that in these references, the crystal system and lattice parameters of $K_2V_8O_{21}$ were not documented. Recently, Tyutyunnik et al. [16] claimed the preparation of $K_2V_8O_{21}$ crystal by heating stoichiometric mixture of K_2CO_3 and V_2O_5 in air at 450 °C for 50 h, and determined its crystal structure by using both neutron and X-ray diffraction data. It was shown that the crystal structure of $K_2V_8O_{21}$ belongs to the monoclinic space group $C2/m$ with the unit cell parameters $a = 14.9402$ Å, $b = 3.61309$ Å, $c = 14.7827$ Å and $\beta = 91.072°$. The structure consists of VO_6 octaheda and VO_5 pyramids forming $[V_8O_{21}]^{2-}$ units running along the b-axis. The K ions are located in tunnels formed by the $[V_8O_{21}]^{2-}$ units [16]. Aleksandrova et al. also reported the synthesis of $K_2V_8O_{21}$ fine particles by heating its precursor in a gas phase-fluidized bed, and the electrochemical properties of the compound were tested. $K_2V_8O_{21}$ exhibits an initial capacity of 90 mAh/g [17,18]. Herein, we developed a simple hydrothermal method to fabricate $K_2V_8O_{21}$ nanobelts from reaction between $KHSO_4$ and V_2O_5 without the use of templates or surfactants. The effects of different experimental parameters on the morphology of the obtained product were also studied.

2. Experimental

All chemicals were analytical grade and used without further purification. In a typical synthesis process, 1.5 mmol V_2O_5 and 3 mmol $KHSO_4$ were dissolved in 85 mL distilled water, and then transferred to a Teflon-lined autoclave with 100 mL capacity. The autoclave was put into an oven and maintained at 200 °C for 24 h. The resulted product was separated by centrifugation, washed several times with distilled water and ethanol, and then dried at 60 °C overnight.

The phase of the obtained products was determined using X-ray diffractometer with Cu Kα radiation (XRD, Rigaku D/max, $\lambda = 1.5406$ Å). The morphology of the sample was examined by scanning electron microscopy (SEM, FEI Sirion). Transmission electron microscopy (TEM) was carried out on a Philips Tecnai 20 microscope operated at 200 kV. The as-prepared nanobelts were dispersed in ethanol aided by ultrasonic treatment. One drop of the suspension was added to a holey carbon film supported on a copper grid for TEM characterization. X-ray photo-electron spectrometry (XPS) of the product was collected on a VG K-Alpha Probe spectrometer (Thermofisher Scientific) with Al Kα radiation as the excitation source.

3. Results and discussion

The phase of the obtained product was examined by XRD, as shown in Fig. 1. The XRD peaks show good agreement with those of $K_2V_8O_{21}$ (PDF No. 24-0906) as reported by Kato et al. [14]. For comparison, the peak positions for standard samples via different methods early reported were also shown in the lower part. Although these early work reported the identical formula of $K_2V_8O_{21}$, their X-ray diffraction patterns are different, which might be due to different synthetic conditions or different raw materials as discussed in Section 1. The strong and sharp peaks indicate that $K_2V_8O_{21}$ is highly crystalline. X-ray photo-electron spectroscopy (XPS) survey spectrum (Fig. 2a) analysis shows that the product consists of K, V and O with K:V:O atomic ratio of about 1:4.2:12.4, which further confirms that the obtained product is $K_2V_8O_{21}$. The V_{2p} region high-resolution XPS spectrum is depicted in Fig. 2b. The bonding energy of $V_{2p\ 3/2}$ and $V_{2p\ 1/2}$ is 516.68 and 524.88 eV, respectively. The bonding energy represents the V^{5+} valence states, and no detectable V^{4+} could be found.

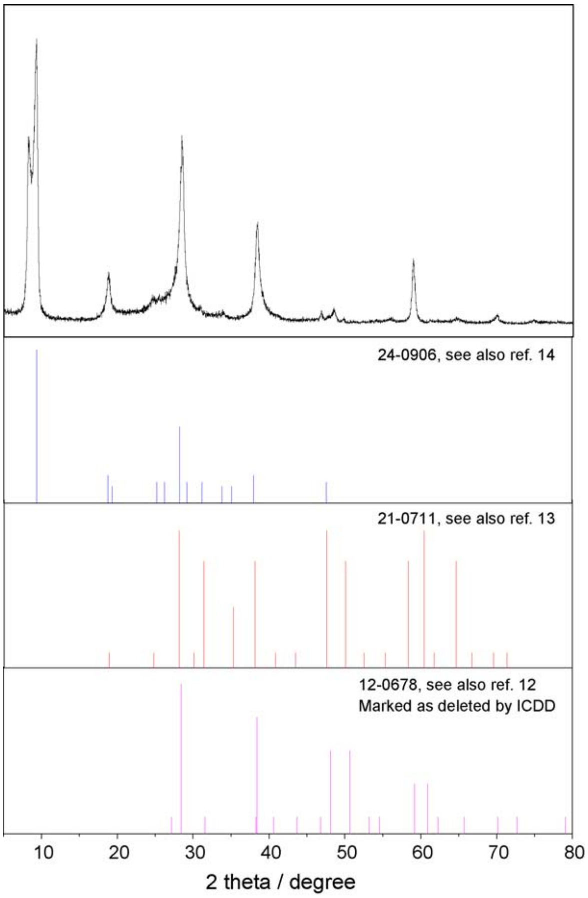

Fig. 1. XRD pattern of the product synthesized at 200 °C for 24 h. The reference angles for the standard sample of $K_2V_8O_{21}$ synthesized from different raw materials are shown at the lower part (PDF2 version 2002).

The product morphology was characterized by scanning electron microscopy. A typical SEM image of the product is shown in Fig. 3a. It is obvious that the obtained product is nanobelts with average width of about 420 nm and length up to a few tens microns. The belt-like characteristics were directly depicted by a slight curled belt shown in Fig. 3b. We can see both the top and side surfaces of the nanobelt with width of about 400 nm and thickness of less than 100 nm. The obtained nanobelts were further characterized by transmission electron

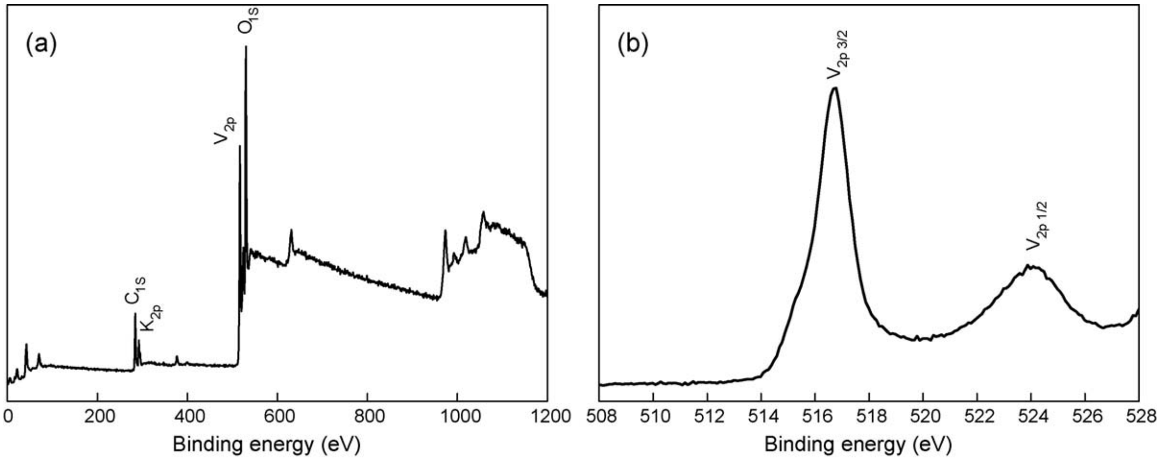

Fig. 2. XPS survey spectrum (a) and high-resolution XPS spectrum of the V_{2p} region (b) of the $K_2V_8O_{21}$ product synthesized at 200 °C for 24 h.

microscopy (TEM). Fig. 4a is a TEM image showing the general morphology of the obtained nanobelts. Most of the nanobelts are transparent to the electron beam, indicating that the thickness of the nanobelts is rather small. The large width-thickness ratio results in the high flexibly of the nanobelts, as suggested by the existence of a wealth of curled nanobelts during TEM observation. Electron diffraction pattern from a single nanobelt in Fig. 4b indicates that the obtained $K_2V_8O_{21}$ nanobelts are highly crystallized, as shown in Fig. 4c. Note that the diffraction pattern is not indexed since the structure of the *present* $K_2V_8O_{21}$ phase was not reported yet. Further work combining XRD refinement and TEM is needed to determine the crystal structure of $K_2V_8O_{21}$ following the methods described in recent work [19,20].

Several batches of experiments were conducted to study the influence of different experimental parameters on the formation of $K_2V_8O_{21}$ nanobelts. The variation of molar ratio of V_2O_5 to $KHSO_4$ from 1:1 to 1:8 does not change the phase of the obtained product except that un-reacted V_2O_5 were found with higher initial V_2O_5 content. With the increase content of $KHSO_4$, the morphology changes from nanobelts to nanowires while the 1D characteristics are all the same, as shown in Fig. 5a. The similar variation tendency was found with the increase of $KHSO_4$ solution concentration from 0.025 to 0.2 mol/L. Fig. 5b shows SEM image of $K_2V_8O_{21}$ nanowires prepared with a high $KHSO_4$ concentration of 0.2 mol/L. A slight decrease of reaction temperature from 200 to 180 °C can also lead to the similar morphology transformation from belt-like to wire-like, as depicted in Fig. 5c. When the reaction temperature is a slightly higher (220 °C), the belt-like characteristics of the obtained product are more apparent (see Fig. 5d).

It has been reported that the use of Na_2SO_4 instead of $NaHSO_4$ leads to the formation of different sodium vanadate nanostructures, i.e. $Na_2V_6O_{16}\cdot 3H_2O$ nanowires or NaV_6O_{16} nanowires [2]. In this work, K_2SO_4 was also used as potassium source under identical experimental conditions, but no precipitations were found after hydrothermal reaction. Thus, it is believed that $KHSO_4$ plays a crucial role in the formation of $K_2V_8O_{21}$ nanobelts. On heating under hydrothermal conditions, $KHSO_4$ might undergo the follow transformation [21]:

$$2KHSO_4 \rightarrow K_2S_2O_7 + H_2O \tag{1}$$

The resulted $[S_2O_7]^{2-}$ might further react with V_2O_5 as follow:

$$4V_2O_5 + [S_2O_7]^{2-} \rightarrow [V_8O_{21}]^{2-} + 2SO_3 \tag{2}$$

where the $[V_8O_{21}]^{2-}$ units containing VO_6 octaheda and VO_5 pyramids are running along the *b*-axis [16]. Potassium ions are situated in the tunnels formed by the $[V_8O_{21}]^{2-}$, and thus $K_2V_8O_{21}$ nanobelts are formed.

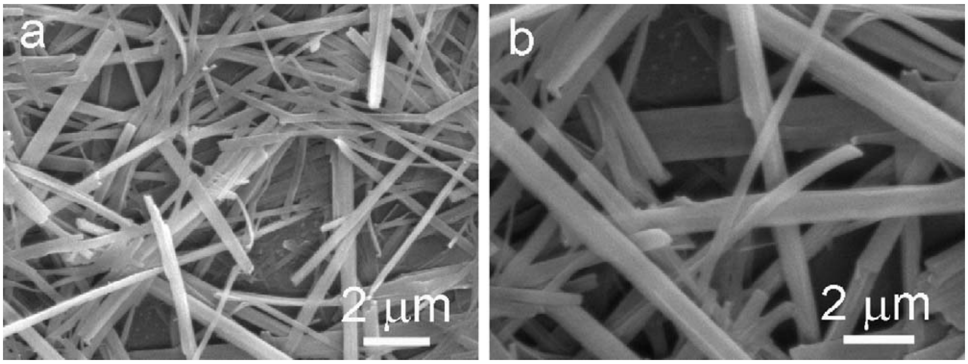

Fig. 3. SEM images of the as-synthesized $K_2V_8O_{21}$ nanobelts synthesized at 200 °C for 24 h: (a) low magnification and (b) high magnification.

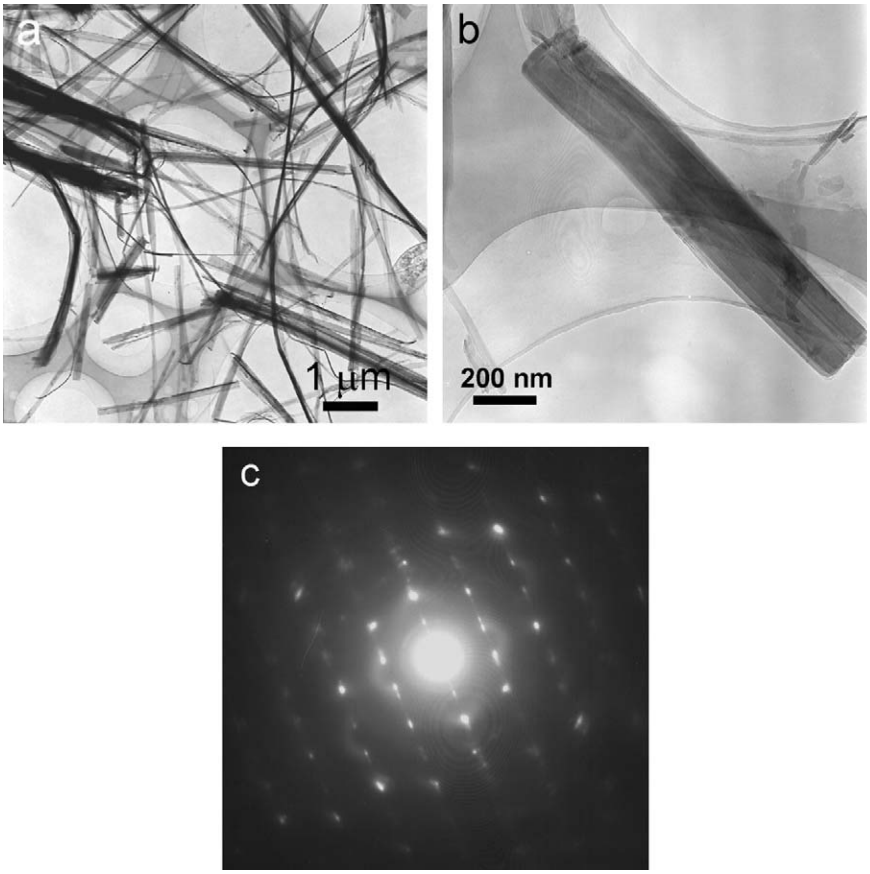

Fig. 4. (a) TEM image of the as-synthesized $K_2V_8O_{21}$ nanobelts synthesized at 200 °C for 24 h showing their general morphology, (b) TEM image of an individual nanobelt and (c) it corresponding SAED pattern.

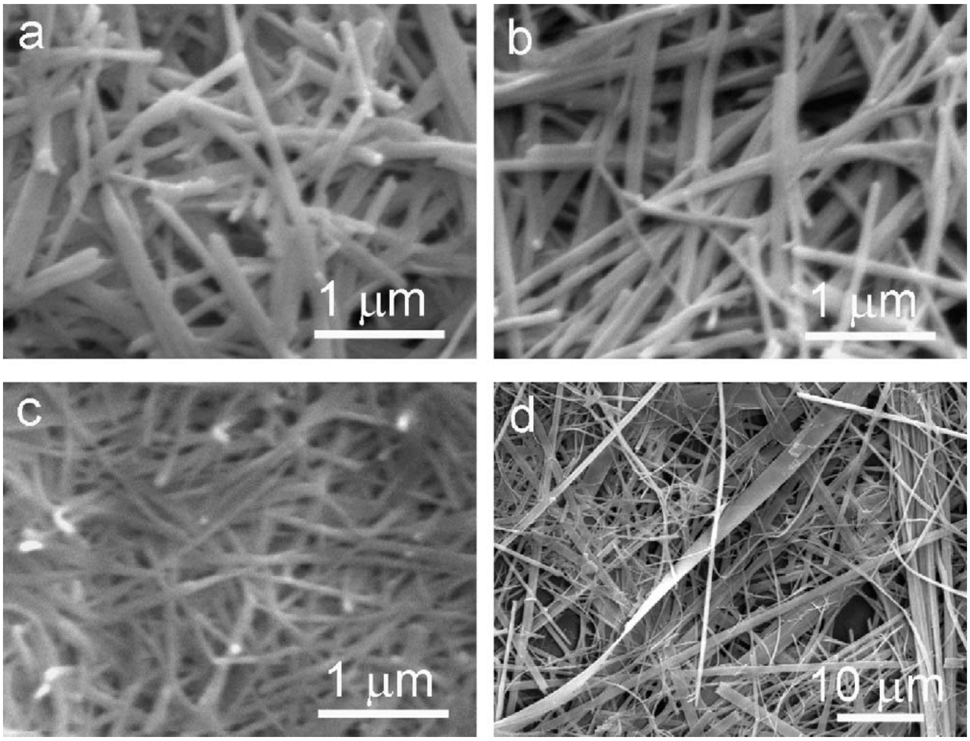

Fig. 5. SEM images of product synthesized at different experimental conditions. (a) V_2O_5:$KHSO_4$ = 1:8, molar ratio; (b) higher $KHSO_4$ concentration of 0.2 mol/L with V_2O_5:$KHSO_4$ = 1:2; (c) T = 180 °C, other experimental conditions are same as the typical one; (d) T = 220 °C, other experimental conditions are same as the typical one.

4. Conclusions

In summary, we have developed a facile hydrothermal route for the synthesis of single-crystal $K_2V_8O_{21}$ nanobelts without using any surfactants or templates. The potassium vanadates 1D nanostructures could be formed within a wide range of experimental parameters with the only restriction of using $KHSO_4$ as potassium source. This solution method offers an alternative strategy for the preparation of $K_2V_8O_{21}$ compared with the conventional solid state synthesis route.

Acknowledgements

This work was financially supported by Natural Science Foundation of China (No. 50902036), Postdoctoral Fellowships from Heilongjiang Province and China Postdoctoral Science Foundation (LBH-Z08112, No. 20080440126, No. 200902381), and Program of Excellent Team at Harbin Institute of Technology.

References

[1] J.G. Yu, J.C. Yu, W.K. Ho, L. Wu, X.C. Wang, J. Am. Chem. Soc. 126 (2004) 3422.
[2] G.T. Zhou, X.C. Wang, J.C. Yu, Cryst. Growth Des. 5 (2005) 969.
[3] J.G. Yu, J.C. Yu, Mater. Chem. Phys. 104 (2007) 362.
[4] L.F. Kong, M.W. Shao, Q. Xie, J.W. Liu, Y.T. Qian, J. Cryst. Growth 260 (2004) 435.
[5] Y. Liu, Y.G. Zhang, J. Du, W.C. Yu, Y.T. Qian, J. Cryst. Growth 291 (2006) 320.
[6] C.J. Mao, X.C. Wu, H.C. Pan, J.J. Zhu, H.Y. Chen, Nanotechnology 16 (2005) 2892.
[7] Y. Liu, Y.G. Zhang, M. Zhang, Y.T. Qian, J. Cryst. Growth 289 (2006) 197.
[8] M. Li, M.G. Shao, H.Z. Ban, H. Wang, H.Z. Gao, Solid State Ions 178 (2007) 775.
[9] Y. Liu, Y.G. Zhang, Y.H. Hu, Y.T. Qian, Chem. Lett. 34 (2005) 146.
[10] J.Q. Yu, A. Kudo, Chem. Lett. 34 (2005) 850.
[11] H.Y. Xu, W.L. He, H. Wang, H. Yan, J. Cryst. Growth 260 (2004) 447.
[12] V.V. Illarionov, R.P. Ozerv, E.V. Kildisheva, J. Inorg. Chem. (USSR) 4 (1956) 780 (see also PDF No. 12-0678).
[13] I. Lukacs, et al. Rev. Roum. Chim. 13 (1968) 95 (see also PDF No. 21-0711).
[14] A. Kato, I. Mochida, T. Seiyama, Anal. Chim. Acta 54 (1971) 168 (See also PDF No. 24-0906).
[15] PDF No. 12-0678, Marked as deleted by ICDD (version 2002) upon the publication of Ref. 14.
[16] A.P. Tyutyunnik, V.G. Zubkov, V.N. Krasil'nikov, G. Svensson, M.J. Sayagués, Solid State Sci. 7 (2005) 37.
[17] A. Aleksandrova, S. Uzunova, B. Banov, A. Momchilov, in: Proceedings of the International Workshop "Advanced Techniques for Energy Sources Investigation and Testing", Sofia, Bulgaria, 4–9 September, (2004), p. 3-1.
[18] A. Aleksandrova, H. Vasilchina, A. Momchilov, B. Banov, in: Proceedings of the International Workshop "Portable and Emergency Energy Sources—from Materials to Systems, Primorsko, Bulgaria, 16–22 September, (2005), p. 2-1.
[19] Z.J. Lin, M.J. Zhuo, Y.C. Zhou, M.S. Li, J.Y. Wang, J. Mater. Res. 21 (2006) 2587.
[20] Z.J. Lin, M.S. Li, Y.C. Zhou, J. Mater. Sci. Technol. 23 (2007) 145.
[21] M.F.R. Fouda, H.I. Saleh, W.H. Hegazy, E.A. Kishar, J. Solid State Chem. 145 (1999) 128.